CLEO CONF95-20
EPS0181
July 19, 1995

Analysis of $\overset{(-)}{D^0} \to K\bar{K}X$ Decays

M. Artuso,[1] M. Gao,[1] M. Goldberg,[1] D. He,[1] N. Horwitz,[1] S. Kopp,[1] G.C. Moneti,[1] R. Mountain,[1] F. Muheim,[1] Y. Mukhin,[1] S. Playfer,[1] S. Stone,[1] X. Xing,[1] J. Bartelt,[2] S.E. Csorna,[2] V. Jain,[2] S. Marka,[2] D. Gibaut,[3] K. Kinoshita,[3] P. Pomianowski,[3] B. Barish,[4] M. Chadha,[4] S. Chan,[4] D.F. Cowen,[4] G. Eigen,[4] J.S. Miller,[4] C. O'Grady,[4] J. Urheim,[4] A.J. Weinstein,[4] F. Würthwein,[4] D.M. Asner,[5] M. Athanas,[5] D.W. Bliss,[5] W.S. Brower,[5] G. Masek,[5] H.P. Paar,[5] J. Gronberg,[6] C.M. Korte,[6] R. Kutschke,[6] S. Menary,[6] R.J. Morrison,[6] S. Nakanishi,[6] H.N. Nelson,[6] T.K. Nelson,[6] C. Qiao,[6] J.D. Richman,[6] D. Roberts,[6] A. Ryd,[6] H. Tajima,[6] M.S. Witherell,[6] R. Balest,[7] K. Cho,[7] W.T. Ford,[7] M. Lohner,[7] H. Park,[7] P. Rankin,[7] J.G. Smith,[7] J.P. Alexander,[8] C. Bebek,[8] B.E. Berger,[8] K. Berkelman,[8] K. Bloom,[8] T.E. Browder,[8*] D.G. Cassel,[8] H.A. Cho,[8] D.M. Coffman,[8] D.S. Crowcroft,[8] M. Dickson,[8] P.S. Drell,[8] D.J. Dumas,[8] R. Ehrlich,[8] R. Elia,[8] P. Gaidarev,[8] M. Garcia-Sciveres,[8] B. Gittelman,[8] S.W. Gray,[8] D.L. Hartill,[8] B.K. Heltsley,[8] S. Henderson,[8] C.D. Jones,[8] S.L. Jones,[8] J. Kandaswamy,[8] N. Katayama,[8] P.C. Kim,[8] D.L. Kreinick,[8] T. Lee,[8] Y. Liu,[8] G.S. Ludwig,[8] J. Masui,[8] J. Mevissen,[8] N.B. Mistry,[8] C.R. Ng,[8] E. Nordberg,[8] J.R. Patterson,[8] D. Peterson,[8] D. Riley,[8] A. Soffer,[8] P. Avery,[9] A. Freyberger,[9] K. Lingel,[9] C. Prescott,[9] J. Rodriguez,[9] S. Yang,[9] J. Yelton,[9] G. Brandenburg,[10] D. Cinabro,[10] T. Liu,[10] M. Saulnier,[10] R. Wilson,[10] H. Yamamoto,[10] T. Bergfeld,[11] B.I. Eisenstein,[11] J. Ernst,[11] G.E. Gladding,[11] G.D. Gollin,[11] M. Palmer,[11] M. Selen,[11] J.J. Thaler,[11] K.W. Edwards,[12] K.W. McLean,[12] M. Ogg,[12] A. Bellerive,[13] D.I. Britton,[13] E.R.F. Hyatt,[13] R. Janicek,[13] D.B. MacFarlane,[13] P.M. Patel,[13] B. Spaan,[13] A.J. Sadoff,[14] R. Ammar,[15] P. Baringer,[15] A. Bean,[15] D. Besson,[15] D. Coppage,[15] N. Copty,[15] R. Davis,[15] N. Hancock,[15] S. Kotov,[15] I. Kravchenko,[15] N. Kwak,[15] Y. Kubota,[16] M. Lattery,[16] M. Momayezi,[16] J.K. Nelson,[16] S. Patton,[16] R. Poling,[16] V. Savinov,[16] S. Schrenk,[16] R. Wang,[16] M.S. Alam,[17] I.J. Kim,[17] Z. Ling,[17] A.H. Mahmood,[17] J.J. O'Neill,[17] H. Severini,[17] C.R. Sun,[17] F. Wappler,[17] G. Crawford,[18] R. Fulton,[18] D. Fujino,[18] K.K. Gan,[18] K. Honscheid,[18] H. Kagan,[18] R. Kass,[18] J. Lee,[18] M. Sung,[18] C. White,[18] A. Wolf,[18] M.M. Zoeller,[18] X. Fu,[19] B. Nemati,[19] W.R. Ross,[19] P. Skubic,[19] M. Wood,[19] M. Bishai,[20] J. Fast,[20] E. Gerndt,[20] J.W. Hinson,[20] T. Miao,[20] D.H. Miller,[20] M. Modesitt,[20] E.I. Shibata,[20] I.P.J. Shipsey,[20] P.N. Wang,[20] L. Gibbons,[21] S.D. Johnson,[21] Y. Kwon,[21] S. Roberts,[21] E.H. Thorndike,[21] T.E. Coan,[22] J. Dominick,[22] V. Fadeyev,[22] I. Korolkov,[22] M. Lambrecht,[22] S. Sanghera,[22] V. Shelkov,[22] T. Skwarnicki,[22] R. Stroynowski,[22] I. Volobouev,[22] and G. Wei[22]

(CLEO Collaboration)

[1]*Syracuse University, Syracuse, New York 13244*
[2]*Vanderbilt University, Nashville, Tennessee 37235*
[3]*Virginia Polytechnic Institute and State University, Blacksburg, Virginia, 24061*
[4]*California Institute of Technology, Pasadena, California 91125*
[5]*University of California, San Diego, La Jolla, California 92093*
[6]*University of California, Santa Barbara, California 93106*
[7]*University of Colorado, Boulder, Colorado 80309-0390*
[8]*Cornell University, Ithaca, New York 14853*
[9]*University of Florida, Gainesville, Florida 32611*
[10]*Harvard University, Cambridge, Massachusetts 02138*
[11]*University of Illinois, Champaign-Urbana, Illinois, 61801*
[12]*Carleton University, Ottawa, Ontario K1S 5B6 and the Institute of Particle Physics, Canada*
[13]*McGill University, Montréal, Québec H3A 2T8 and the Institute of Particle Physics, Canada*
[14]*Ithaca College, Ithaca, New York 14850*
[15]*University of Kansas, Lawrence, Kansas 66045*
[16]*University of Minnesota, Minneapolis, Minnesota 55455*
[17]*State University of New York at Albany, Albany, New York 12222*
[18]*Ohio State University, Columbus, Ohio, 43210*
[19]*University of Oklahoma, Norman, Oklahoma 73019*
[20]*Purdue University, West Lafayette, Indiana 47907*
[21]*University of Rochester, Rochester, New York 14627*
[22]*Southern Methodist University, Dallas, Texas 75275*

(July 19, 1995)

Abstract

Using 2.7 fb^{-1} of data taken with the CLEO II detector, we have studied the decays of the D^0 to: K^+K^-, $K^0\bar{K}^0$, $K^0_SK^0_SK^0_S$, $K^0_SK^0_S\pi^0$, $K^+K^-\pi^0$.

---

*Permanent address: University of Hawaii at Manoa

I. INTRODUCTION

Since the discovery of charmed mesons in 1976 many measurements have been made of their decay properties. In particular, detailed measurements of rare exclusive decay modes have provided a powerful way to probe the details of charmed decays such as the contributions of W-exchange diagrams and final-state interactions, and are thus an important means of probing the interplay between the weak and strong interactions. The CLEO II experiment is now reaching a level of sensitivity which allows for the systematic study of several rare decay modes of the D^0. We report on the measurements of the decay rates of several CP eigenstate decay modes which involve final states containing two or more kaons.

A. K^+K^-

This decay mode is Cabibbo suppressed. Some of the Feynman diagrams leading to this final state are shown in Figure 1. It has yet to be understood why the ratio, $B(D^0 \to K^+K^-)/B(D^0 \to \pi^+\pi^-)$, is much greater than one. These two decay modes both proceed through similar diagrams so that the expected ratio is 1 without SU(3) flavor symmetry breaking. Solutions proposed to explain the deviation from 1 include SU(3) symmetry breaking effects [1], final-state interactions [2–4], and/or QCD sum rules [5]. A different approach is to invoke penguin diagrams which interfere constructively with the spectator decay for KK but destructively for $\pi\pi$ [6]. We will improve measurements of these decays and of their ratio to help resolve this puzzle.

Table I lists the major theories and their predictions for the $D^0 \to K^+K^-$ branching ratio and table II summarizes current measurements.

TABLE I. The present predictions for the KK branching ratios

Theory models	Branching ratio(%)	
	K^+K^-	$K^0\bar{K}^0$
Spectator Model [7]	0.14	0
WSB Model [1]	0.56	–
CC Model [2]	0.25±0.06	0
FSI Model [4]	0.39	0.13
I. Bigi [8]	0.6	–
QCD sum rule [5]	0.3	0
X. Y. Pham [9]	–	0.3

B. $K^0\bar{K}^0$

This channel is interesting for two reasons. The first is that the $D^0 \to K^0\bar{K}^0$ decay channel allows us to study the effect of final state interactions. The $D^0 \to K^0\bar{K}^0$ decay is expected to occur primarily via the W exchange diagrams shown in Figure 2. Since

TABLE II. The present measurements for the KK branching ratios

Measurements	Branching ratio(%)	
	K^+K^-	$K^0\bar{K}^0$
MARK2 79 [10]	0.45±0.12*	
MARK3 85 [11]	0.49±0.07±0.05*	
E400 88 [12]		0.10±0.07
CLEO 90 [13]	0.49±0.04±0.03	0.13±0.07
ARGUS 90 [14]	0.40±0.08±0.04*	
E691 91 [15]	0.43±0.04±0.04*	
NA14 91 [16]	0.64±0.20*	
E687 92 [17]	0.55±0.11±0.04*	
OMEG 92 [18]	0.43±0.12±0.06*	
E687 94 [19]	0.44±0.03±0.04*	
E687 94 [20]		0.21±0.07±0.07†
World Average 94 [21]	0.454±0.029	0.11 ±0.04

* We have used $B(D^0 \to K^-\pi^+) = 4.01 \pm 0.14\%$ [21]. † We have used $B(D^0 \to \bar{K}^0\pi^+\pi^-) = 5.3 \pm 0.9\%$ [21].

the Cabibbo factors have opposite signs, we might expect an exact cancelation of the two amplitudes in the four-quark model. In the standard six-quark model the difference between the two amplitudes is tiny, we thus might expect the branching fraction for the decay to be very small. However, a recent calculation predicts a relatively large branching fraction due to final state rescattering with a branching ratio of $B(D^0 \to K^0\bar{K}^0) = 0.3\%$ within the standard model [9]. If the branching ratio turns out to be larger than 0.3%, then this decay is impossible to understand within the framework of the standard theory. Thus, this channel provides a way of testing the standard theory. Table I and table II list the major theories and their predictions for the $D^0 \to K^0\bar{K}^0$ branching ratio and the current measurements respectively.

The other reason that this decay mode is particularly important is that it is part of the isospin analysis of $D \to KK$ decays. It will be interesting to compare the results of this analysis with the $D \to \pi\pi$ isospin analysis of CLEO II [22].

C. $K^0_SK^0_SK^0_S$

Since this decay was first observed by the ARGUS Collaboration ($B(D^0 \to K^0_SK^0_SK^0_S) = 0.09 \pm 0.04\%$) [14], there have been two other measurements, made by CLEO 1.5 ($B(D^0 \to K^0_SK^0_SK^0_S) = 0.11 \pm 0.03\%$) [23] and by E687 ($B(D^0 \to K^0_SK^0_SK^0_S) = 0.19 \pm 0.06 \pm 0.04\%$) [20]. This channel is Cabibbo allowed but cannot be made via a simple spectator process. Instead, its formation requires the popping of an $s\bar{s}$ pair (Fig 3) and so its existence can be an indication that either W exchange or final state interactions are taking place.

D. $K_S^0 K_S^0 \pi^0$

There has been no previous measurement of this decay rate. This channel is Cabibbo-suppressed and involves the popping of $d\bar{d}$ pairs (Fig 4). Again, we cannot form it via a simple spectator process. So, again, its existence might indicate that either Cabibbo suppressed W exchange or final state interactions are important. This channel can include a contribution from resonant $K^{*0} K_S^0$ production. It is also interesting to compare this branching ratio with that of the Cabibbo favored $K_S^0 K_S^0 K_S^0$ channel.

E. $K^+ K^- \pi^0$

There has been no previous measurement of this decay rate. This decay is Cabibbo-suppressed (Fig 5). This channel can include contributions from resonant $K^{*+}K^-$, $K^{*-}K^+$ and $\phi\pi^0$ production. This result can be compared with that of the double Cabibbo suppressed decay mode of $K^+\pi^-\pi^0$ measured at CLEO II [24].

II. ANALYSIS

A. Data Sample

We use data taken with the CLEO II detector at the Cornell Electron Storage Ring. The data set used in this analysis corresponds to 2.7 fb^{-1} of data taken on and just below the $\Upsilon(4S)$ resonance.

The CLEO II detector [25] is designed to detect both charged and neutral particles with excellent resolution and efficiency. The detector consists of a charged particle tracking system surrounded by a time-of-flight (TOF) scintillation system and an electromagnetic shower detector consisting of 7800 thallium-doped cesium iodide crystals. In the "good barrel" region, defined as the region where the angle of the shower with respect to the beam axis lies between 45^o and 135^o, the r.m.s. resolution in energy is given by $\delta E/E(\%) = 0.35/E^{0.75} + 1.9 - 0.1E, (E$ in GeV). The tracking system, time-of-flight scintillators, and calorimeter are installed inside a 1.5 T superconducting solenoidal magnet. Immediately outside the magnet are iron and chambers for muon detection. The momentum resolution of the tracking system is given by $(\delta p/p)^2 = (0.0015p)^2 + (0.005)^2$, where p is in GeV/c. Ionization loss information (dE/dx) is also provided.

B. Procedure

Requiring that the D's used in this analysis come from D^* decays to $D\pi$ gives us a much clearer D signal since the $D^* - D$ mass difference distribution is sharply peaked for true events. We use a $D^{*\pm}$ tag for all the channels except the $K_S^0 K_S^0 K_S^0$ channel. Since this latter channel is kinematically restricted, we can see a clean signal without this tag. For the $K^0\bar{K}^0$ decay channel we add the D^{*0} tag so as to increase the number of events even though the π^0

resolution is not as good as that for the charged pions. Table III summarizes the tags and normalization modes used.

To get the Monte Carlo efficiencies, we generated 20,000 events in each channel.

In this analysis, we do not consider any charge dependent effect (any CP asymmetries [26] are very small). The following analyses sum both charges.

TABLE III. Tags and normalization modes

Channel	Tag	Normalization mode
K^-K^+	$D^{*\pm}$	$K^-\pi^+$
$K^0\bar{K}^0$	$D^{*\pm}, D^{*0}$	$\bar{K}^0\pi^+\pi^-$
$K^0_SK^0_SK^0_S$	No tag	$\bar{K}^0\pi^+\pi^-$
$K^0_SK^0_S\pi^0$	$D^{*\pm}$	$\bar{K}^0\pi^+\pi^-$
$K^-K^+\pi^0$	$D^{*\pm}$	$K^-\pi^+\pi^0$

C. The Initial Selection

In this analysis, we first reconstruct the D^0 decays. Details of this reconstruction can be found in the sections on each specific decay mode. We then combine the D candidate with a pion to reconstruct a $D^{*+} \to D^0\pi^+$ decay. This pion is denoted as the soft pion. In this reconstruction, the dominant source of background is combinatorics – random combinations of tracks which accidentally give the expected mass. This background can be either due to a correctly reconstructed D which is combined with a wrong soft pion, or a fake D in which at least one of the decay products is misidentified, combined with the correct soft pion from the D^* decay.

In most of the background events, a wrong soft pion was used to form the D^*. We determine the number of these events by fitting the $\Delta M (\equiv M_{D^{*+}} - M_{D^0})$ background distribution and integrating under the curve in the signal region. The functional form used is

$$a(\Delta M - m_{\pi^+})^{0.5} + b(\Delta M - m_{\pi^+})^{1.5} + c(\Delta M - m_{\pi^+})^{2.5}$$

where the first term is from a non-relativistic model of phase space, and the second and third terms are the first and second order relativistic corrections to the non-relativistic model, respectively.

To get the number of true signal events, we count the number of events in the signal region and subtract off the number of background events that are in the same region in the D^0 invariant mass plot. The D^0 signal region is defined to be within 3σ of the fitted mass, determined using a Gaussian fit of the real data or if there are too few signal events by using Monte Carlo. For rare decay modes one advantage of this procedure compared with simply fitting the D^0 mass plot is that it avoids the necessity of fitting the complicated shape of the combinatorial background. Studies show that the results of this method are consistent with that of the fitting method within the statistical errors. For the normalization modes, we fit the D^0 mass plot using Gaussian and Chebyshev polynomial functions since they have a large number of events as a relatively small background.

The maximum D^* decay momentum for D^*'s from B meson decay is 2.25 GeV/c in the B meson rest frame. We restrict this study to D^* continuum production. This gives the greatest reconstruction efficiencies. D^* candidates are therefore required to have a momentum greater than 2.45 GeV/c which is similar to a cut of x_p greater than 0.5, where $x_p = p/p_{max}$.

III. MEASUREMENTS AND RESULTS

A. K^+K^-

In this channel we optimize the cuts on track quality. We also apply a cut on the kaon momentum of $P_{K^\pm} > 0.3$ GeV/c, and require that $|\cos\theta_{\mathrm{K}^\pm}| < 0.8$ where the angle $\theta_{K^\pm}$ is the angle between the $K^\pm$ momentum in the D^0 rest frame and the D^0 laboratory momentum. Since the D^0, K^+ and K^- are spin-less, the D^0 decays isotropically, whereas the background shows a peak at $|\cos\theta_{\mathrm{K}^\pm}| \approx 1.0$.

Using these cuts, we obtain the D^0 mass spectrum shown in Figure 6. For this channel the signal region is between 1.84 and 1.89 GeV/c^2. The number of events in the D^0 signal region is 2785 and the number of background events coming from the mass difference sideband region is 1119.0±20.1.

At this stage, there is the possibility that backgrounds from other charm decay modes such as $K^-\pi^+\pi^0$ are also present in the D signal region even if most of these events lie outside it. To determine this background, we use a Monte Carlo simulation of continuum hadron production and decay followed by a full simulation of the signals the particles produced in the detector. The K^+K^- invariant mass distribution of these events excluding true $D^0 \to K^+K^-$ decays is shown superimposed on the data in Figure 6, where the background from the ΔM sideband was subtracted for Monte Carlo events. The normalization of the simulated events is absolutely determined from the luminosity. We find 563.7±40.1 background events from this source. As shown in Figure 7, the backgrounds are well-understood. After subtracting all the backgrounds, we find $N(K^+K^-)$= 1102.3±69.3 for $D^0 \to K^+K^-$.

To get the branching ratio, we use $D^0 \to K^-\pi^+$ as the normalization mode:

$$\frac{B(D^0 \to K^+K^-)}{B(D^0 \to K^-\pi^+)} = \left[\frac{N(K^+K^-)}{\epsilon_{K^+K^-}}\right]\left[\frac{\epsilon_{K^-\pi^+}}{N(K^-\pi^+)}\right]$$

where N is the number of observed events in each case and ϵ is the corresponding reconstruction efficiency which includes the D^{*+} reconstruction efficiency as determined from Monte Carlo. The detector efficiencies from MC are $\epsilon_{K^+K^-} = 22.88 \pm 0.34\%$ and $\epsilon_{K^-\pi^+} = 37.72 \pm 0.49\%$. We observe $N(K^-\pi^+) = 15633 \pm 202$ for $D^0 \to K^-\pi^+$. Using $B(D^0 \to K^-\pi^+) = 3.91 \pm 0.08 \pm 0.17\%$ [27], we measure $B(D^0 \to K^+K^-) = 0.455 \pm 0.029\%$.

As a systematic check of the effect of our event selection cuts, we extract the signal yields with the mass difference cut, D^* momentum cut and the decay angle cut individually tightened by 20% of their nominal values. We consider the worst case as the systematic error due to the variations of the yield with different cuts, giving a contribution to the systematic error of 4.8%. The variations of the yield with different sideband subtractions are consistent within statistical errors. The systematic errors due to united Monte Carlo statistics and the uncertainty in the normalization branching fraction are 2.0% and 4.8%

respectively. This gives a total systematic error of 7.1%. We measure $B(D^0 \to K^+K^-) = 0.455 \pm 0.029 \pm 0.032\%$.

B. $K^0\bar{K}^0$

We study the $K^0_SK^0_S$ component of this decay. Due to the small number of events, we use not only a $D^{*\pm}$ tag but also the D^{*0} tag.

In this channel the dominant sources of backgrounds are from non-resonant $K^0_S\pi^+\pi^-$ and $\pi^+\pi^-\pi^+\pi^-$ production. To reduce feed-through from $D^0 \to K^0_S\pi^+\pi^-$, where the $\pi^+\pi^-$ fakes a K^0_S or from $D^0 \to \pi^+\pi^-\pi^+\pi^-$, where the four pions fake 2 K^0_S's, we first reconstruct K^0_S mesons from $\pi^+\pi^-$ pairs with an invariant mass within 0.0108 GeV/c^2($\sim 3\sigma$) of the nominal K^0_S mass and a vertex displaced at least 5 mm from the beam position. We also apply $|cos_{\theta_{K^0_S}}| <0.8$, where the angle $\theta_{K^0_S}$ is the angle between the K^0_S momentum in the D^0 rest frame and the D^0 laboratory momentum.

To get the branching ratio, we use

$$\frac{B(D^0 \to K^0\bar{K}^0)}{B(D^0 \to \bar{K}^0\pi^+\pi^-)} = \frac{1}{B(K^0_S \to \pi^+\pi^-)}\left[\frac{N(K^0_SK^0_S)}{\epsilon_{K^0_SK^0_S}}\right]\left[\frac{\epsilon_{K^0_S\pi^+\pi^-}}{N(K^0_S\pi^+\pi^-)}\right]$$

where N is the number of observed events in each case and ϵ is the corresponding reconstruction efficiency. Because $B(D^0 \to K^0\bar{K}^0) = 2B(D^0 \to K^0_SK^0_S)$, the factors $B(\bar{K}^0\pi^+\pi^- \to K^0_S\pi^+\pi^-)$ and $B(K^0\bar{K}^0 \to K^0_SK^0_S)$ become equal and cancel in the above relation [13]. We use $B(D^0 \to \bar{K}^0\pi^+\pi^-) = 5.3 \pm 0.6\%$ and $B(K^0_S \to \pi^+\pi^-) = 68.61 \pm 0.28\%$ [21].

1. $D^{*\pm}$ tag

Using the $D^{*\pm}$ tag, we obtain the D^0 mass spectrum shown in Figure 8. For this tag the signal region is between 1.84 and 1.89 GeV/c^2. The number of events in the D^0 signal region is 12 and the number of background events coming from the mass difference sideband region is 1.1±0.3. So, we get $N(K^0_SK^0_S) = 10.9 \pm 3.5$. The detection efficiencies determined by MC are $\epsilon_{K^0_SK^0_S} = 8.46 \pm 0.21\%$ and $\epsilon_{K^0_S\pi^+\pi^-} = 13.36 \pm 0.31\%$. We get $N(K^0_S\pi^+\pi^-) = 3184 \pm 102$, giving $B(D^0 \to K^0\bar{K}^0) = 0.042 \pm 0.013\%$ for this tag.

2. D^{*0} tag

We use a stronger mass difference cut $|M_{D^{*0}} - M_{D^0} - 0.1423| < 0.0022$ GeV ($\sim 2.5\sigma$) for the D^0 tag since the π^0 momentum resolution is worse than that of the charged tracks. We obtain the D^0 mass spectrum shown in Figure 9. For this tag the signal region is between 1.84 and 1.89 GeV/c^2. The number of events in the D^0 signal region is 9 and the number of background events coming from mass difference sideband region is 1.1±0.4. So, we get $N(K^0_SK^0_S) = 7.9 \pm 3.0$. The detection efficiencies determined from MC are $\epsilon_{K^0_SK^0_S} = 3.54 \pm 0.15\%$ and $\epsilon_{K^0_S\pi^+\pi^-} = 6.78 \pm 0.57\%$. We get $N(K^0_S\pi^+\pi^-) = 1327 \pm 89$, and we measure $B(D^0 \to K^0\bar{K}^0) = 0.088 \pm 0.034\%$ for this tag.

Figure 10 shows the sum of the $D^{*\pm}$ tag and the D^{*0} tag data.

As a systematic check of the effect of our event selection cuts, we extract the signal yields with the mass difference cut, D^* momentum cut, the decay angle cut, the vertex cut and the K_S^0 mass cut individually tightened by 20% of their nominal values. We consider the worst case as the systematic error due to the variations of the yield with different cuts. We also studied a sideband region in the K_S^0's mass domain to determine the non-resonant $\pi^+\pi^-$ background. Results indicate that there are 0.1 non-resonant $\pi^+\pi^-$ background events for the $D^{*\pm}$ tag and none for the D^{*0} tag. Another systematic error involved in measuring the K_S^0's is the K_S^0's finding efficiency in CLEO II detector. This error on this efficiency is 5% per K_S^0. A summary of the systematic errors for this channel is given in table IV.

TABLE IV. Summary of systematic errors for the $K^0\bar{K}^0$ channel

	Systematic errors(%)	
Source of error	$D^{*\pm}$ tag	D^{*0} tag
Signal yield (cuts)	23.8	22.7
Non-resonant $\pi^+\pi^-$ background	0.9	0.0
K_S^0's finding efficiency	5.0	5.0
Monte Carlo statistics	3.4	9.4
PDG branching fraction	11.3	11.3
Total	27.1	27.5

The final results are $B(D^0 \to K^0\bar{K}^0) = 0.042 \pm 0.013(stat) \pm 0.011(sys)\%$ for the $D^{*\pm}$ tag and $B(D^0 \to K^0\bar{K}^0) = 0.088 \pm 0.034(stat) \pm 0.024(sys)\%$ for the D^{*0} tag. These two results are consistent within errors. Finally, we combine the data from the two tags. The combined branching ratio is $B(D^0 \to K^0\bar{K}^0) = 0.048 \pm 0.012(stat) \pm 0.013(sys)\%$.

C. $K_S^0K_S^0K_S^0$

This particular mode is essentially background free since it is kinematically so restricted, so we do not require any D^* tag. Three K_S^0's have to be observed, which makes the efficiency rather low, so the K_S^0 cuts used for this decay are looser than those we use for the other analyses described in this paper.

We first reconstruct K_S^0 mesons from $\pi^+\pi^-$ pairs with an invariant mass within 0.0108 GeV/c^2($\sim 3\sigma$) of the nominal K_S^0 mass and a vertex displaced at lease 2 mm from the beam position. We plot the $K_S^0K_S^0K_S^0$ invariant mass for $P_{D^0} > 2.48$ GeV/c which is similar to requiring x_p greater than 0.5. This $K_S^0K_S^0K_S^0$ invariant mass distribution is fitted by a Gaussian and Chebyshev polynomial order 1. We get a signal of $N(K_S^0K_S^0K_S^0) = 61.0 \pm 8.4$(Figure 11).

To get the branching ratio, we use

$$\frac{B(D^0 \to K_S^0K_S^0K_S^0)}{B(D^0 \to \bar{K}^0\pi^+\pi^-)} = \frac{1}{B(K_S^0 \to \pi^+\pi^-)^2}\left[\frac{N(K_S^0K_S^0K_S^0)}{\epsilon_{K_S^0K_S^0K_S^0}}\right]\left[\frac{\epsilon_{K_S^0\pi^+\pi^-}}{2N(K_S^0\pi^+\pi^-)}\right]$$

where N is the number of observed events in each case and ϵ is the corresponding reconstruction efficiency. The detection efficiencies determined from MC are $\epsilon_{K^0_S K^0_S K^0_S} = 5.20 \pm 0.16\%$ and $\epsilon_{K^0_S \pi^+\pi^-} = 16.78 \pm 0.40\%$. We get $N(K^0_S\pi^+\pi^-) = 14993 \pm 457$. Using $B(K^0_S \to \pi^+\pi^-) = 68.61 \pm 0.28\%$ and $B(D^0 \to \bar{K}^0\pi^+\pi^-) = 5.3 \pm 0.6\%$ [21], we measure $B(D^0 \to K^0_S K^0_S K^0_S) = 0.074 \pm 0.010\%$. This measurement reduces the statistical error significantly compared with the previous two measurements [14,23].

As a systematic check, we study the variations of the yield with different cuts tightened by 20% of their nominal values. The systematic error due to this source is 20.3%. The systematic error due to the K^0_S's finding efficiency in the CLEO II detector is 7.1% for two K^0_S. The systematic errors due to the Monte Carlo statistics and normalization branching fraction are 3.9% and 11.3% respectively. So, the total systematic error is 24.6%. Finally, we measure $B(D^0 \to K^0_S K^0_S K^0_S) = 0.074 \pm 0.010 \pm 0.018\%$.

D. $K^0_S K^0_S \pi^0$

In this decay mode, there are very few events and the background is large. So, we use the same tight cuts on the K^0_S's as we do for the $K^0_S K^0_S$ channel.

We detect π^0's by their decays to $\gamma\gamma$. Candidate π^0's are formed by taking two-photon combinations. The individual photons appear as clusters in the CsI calorimeter. The energy of each cluster has to be at least 30 MeV and the di-photon combination must have at least one photon in the higher resolution portion of the calorimeter ($|\cos(\theta)| < 0.71$, where θ is the angle with respect to the beam axis). We reject all photons matched to charged tracks in the central detector. We use the $P_{\pi^0} > 0.2$ GeV/c and $M_{\pi^0} < 3\sigma$.

Using these cuts, we get the number of D^0 events in the mass difference signal region and the number of D^0 events in the mass difference sideband region (Figure 12). For this channel the signal region is between 1.82 and 1.90 GeV/c^2. The number of signal events is 35 and the number of background events in same region is 24±2. So, we get $N(K^0_S K^0_S \pi^0) = 11 \pm 6$. The signal is within 3σ of the statistical error. We will, therefore, calculate an upper limit on the branching fraction.

To get a branching ratio, we use

$$\frac{B(D^0 \to K^0_S K^0_S \pi^0)}{B(D^0 \to \bar{K}^0\pi^+\pi^-)} = \frac{1}{B(K^0_S \to \pi^+\pi^-)} \left[\frac{N(K^0_S K^0_S \pi^0)}{\epsilon_{K^0_S K^0_S \pi^0}}\right] \left[\frac{\epsilon_{K^0_S \pi^+\pi^-}}{2N(K^0_S\pi^+\pi^-)}\right]$$

where N is the number of the observed events in each case and ϵ is the corresponding reconstruction efficiency. The detection efficiencies determined from MC are $\epsilon_{K^0_S K^0_S \pi^0} = 5.34 \pm 0.17\%$ and $\epsilon_{K^0_S \pi^+\pi^-} = 13.36 \pm 0.31\%$. All the systematic errors are negligible given the size of the statistical error. So, the systematic uncertainties have not been included. We get $N(K^0_S\pi^+\pi^-) = 3184 \pm 102$. Using $B(K^0_S \to \pi^+\pi^-) = 68.61 \pm 0.28\%$ and $B(D^0 \to \bar{K}^0\pi^+\pi^-) = 5.3 \pm 0.6\%$ [21], we measure $B(D^0 \to K^0_S K^0_S \pi^0) = 0.033 \pm 0.018\%$ or $B(D^0 \to K^0_S K^0_S \pi^0) < 0.063\%$ at 90% confidence level.

E. $K^+K^-\pi^0$

Finally, we measure $D^0 \to K^+K^-\pi^0$. For this decay mode, the misidentification of a π^+ as a K^+ is the largest source of background. The major source of this background is from the following Cabibbo favored decays($D^{*+} \to D^0 + \pi^+$ followed by $D^0 \to K^-\pi^+\pi^0$). The branching ratio($B(D^0 \to K^-\pi^+\pi^0) = 11.5 \pm 0.6 \pm 2.4\%$ [28]) for this background is very large. So, in order to select the $K^+K^-\pi^0$ decay mode and reduce the $K^-\pi^+\pi^0$ background, we change a kaon candidate assignment to a pion and calculate the D^0 mass ($M_{K^-\pi^+\pi^0}$). If $M_{K^-\pi^+\pi^0}$ is within 3σ of the nominal D^0 mass, we eliminate the combination. We also use tighter cuts than those of other decay modes such as $P_{D^{*+}} > 2.93$ GeV/c which is similar to requiring x_p greater than 0.6.

We require that the normalized difference between the expected and measured dE/dx for the kaon hypothesis be within 2σ for both kaons. We also require $P_{K^\pm} > 0.3$ GeV/c for clean particle ID.

As for π^0, we use the same π^0 cuts used in $K^0_S K^0_S \pi^0$ analysis except for $P_{\pi^0} > 0.4$ GeV/c and $M_{\pi^0} < 2\sigma$.

Using these cuts, we obtain the D^0 mass spectrum after doing the normalized mass difference sideband subtraction shown in Figure 13. It is fitted by a Gaussian and a Chebyshev polynomial of order 2. We get a signal of $N(K^+K^-\pi^0) = 151 \pm 42$, and $\epsilon_{K^+K^-\pi^0}$=9.25$\pm$0.27%.

To get the branching ratio, we use

$$\frac{B(D^0 \to K^+K^-\pi^0)}{B(D^0 \to K^-\pi^+\pi^0)} = \left[\frac{N(K^+K^-\pi^0)}{\epsilon_{K^+K^-\pi^0}}\right]\left[\frac{\epsilon_{K^-\pi^+\pi^0}}{N(K^-\pi^+\pi^0)}\right].$$

We get $\epsilon_{K^-\pi^+\pi^0} = 4.95 \pm 0.25\%$. We also get $N(K^-\pi^+\pi^0) = 8680 \pm 209$. Using $B(D^0 \to K^-\pi^+\pi^0) = 11.5 \pm 0.6 \pm 2.4\%$ [28], we get the $B(D^0 \to K^+K^-\pi^0) = 0.107 \pm 0.030\%$. All the other systematic errors are negligible given the size of the statistical error.

IV. SUMMARY AND CONCLUSIONS

We have investigated D^0 decays to several rare final states which have two or three kaons in the final state. The figures 14, 15 and 16 show the previous measurements and our results for K^+K^-, $K^0\bar{K}^0$ and $K^0_S K^0_S K^0_S$ respectively. Table V gives the final summary of our results, where the first error is statistical and the second is the estimate of our systematic uncertainty. The K^+K^-, $K^0\bar{K}^0$ and $K^0_S K^0_S K^0_S$ results reduce the errors significantly compared to earlier measurements. We have made the first measurement of an upper limit on the $K^0_S K^0_S \pi^0$ branching fraction. We have made the first measurement of the $K^+K^-\pi^0$ branching fraction.

ACKNOWLEDGMENTS

We gratefully acknowledge the effort of the CESR staff in providing us with excellent luminosity and running conditions. This work was supported by the National Science Foundation, the U.S. Department of Energy, the Heisenberg Foundation, the Alexander von

TABLE V. Summary of the branching fractions, where the first error is statistical and the second is the estimate of our systematic uncertainty.

Channel	Theory(%)	B(%)	World Average(%)
K^+K^-	0.14∼0.6	$0.455 \pm 0.029 \pm 0.032$	0.454 ± 0.029
$K^0\bar{K}^0$	0∼0.3	$0.048 \pm 0.012 \pm 0.013$	0.11 ± 0.04
$K^0_S K^0_S K^0_S$		$0.074 \pm 0.010 \pm 0.018$	0.089 ± 0.025
$K^0_S K^0_S \pi^0$		< 0.063 @90% CL	
$K^+K^-\pi^0$		0.107 ± 0.030	

Humboldt Stiftung, the Natural Sciences and Engineering Research Council of Canada, and the A.P. Sloan Foundation.

REFERENCES

[1] M. Bauer *et al*, Z. Phys. C **34** 103 (1987).
[2] L. L. Chau, Phys. Rep. **95** (1983).
[3] A. N. Kamal *et al*, Phys. Rev. D **35** 3515 (1987); D **36** 3510 (1987); L. L. Chau *et al*, Phys. Lett. B **280** 281 (1992).
[4] A. Czarnecki *et al*, Z. Phys. C **54** 411 (1992)
[5] B. Yu and M. Shifman, Sov. J. Nucl. Phys. **45** 522 (1987).
[6] M. Gluck, Phys. Lett. B **88** 145 (1979); J. Finjord, Nucl. Phys. B **181** 74 (1981).
[7] N. Cabibbo and L. Maiani, Phys. Lett. B **73** 418 (1978).
[8] I. I. Bigi, Nucl. Phys. B **281** 41 (1987).
[9] X. Y. Pham, Phys. Lett. B **193** 331 (1987).
[10] Abrams *et al*, Phys. Rev. Lett. **43** 481 (1979).
[11] R. M. Baltrusait *et al*, Phys. Rev. Lett. **55** 150 (1985).
[12] J. P. Cumalat *et al*, Phys Lett. B **210** 253 (1988).
[13] J. Alexander *et al*, Phys. Rev. Lett. **65** 1184 (1990).
[14] H. Albercht *et al*, Z. Phys. C **46** 9 (1990).
[15] J. C. Anjos *et al*, Phys. Rev. D **44** R3371 (1991).
[16] M. P. Alvarez *et al*, Z. Phys. C **50** 11 (1991).
[17] P. L. Frabetti *et al*, Phys. Lett. B **281** 167 (1992).
[18] M. Adamovich *et al*, Phys. Lett. B **280** 163 (1994).
[19] P. L. Frabetti *et al*, Phys. Lett. B **321** 295 (1994).
[20] P. L. Frabetti *et al*, Phys. Lett. B **340** 254 (1994).
[21] Particle Data Group, Phys. Rev. D **50** 1173 (1994).
[22] M. Selen *et al*, Phys. Rev. Lett. **71** 1973 (1993).
[23] R. Ammar *et al*, Phys. Rev. D **44** 3383 (1991).
[24] G. Crawford *et al*, ICHEP94, Ref. GLS0458 (1994).
[25] Y. Kubota *et al*, Nucl. Instrum. Methods Phys. Res., Sect. A **320**, 66 (1992).
[26] J.Bartelt *et al*, CLNS95/1333 (1995).
[27] D. S. Akerib *et al*, Phys. Rev. Lett. **71** 3070 (1993).
[28] K. Kinoshita *et al*, Phys. Rev. D **43** 2837 (1991).

FIGURES

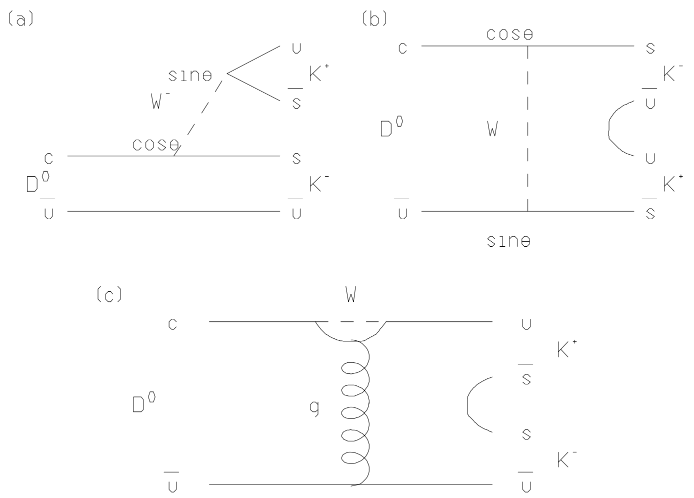

FIG. 1. The significant Feynman diagrams for $D^0 \to K^+K^-$: (a) quark decay, (b) annihilation and (c) penguins.

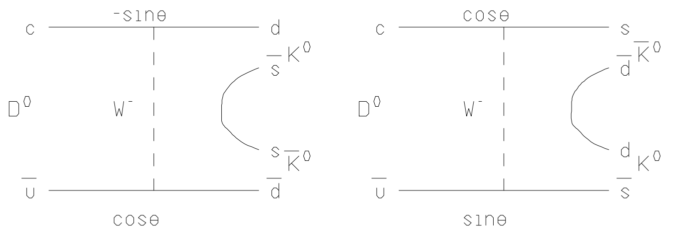

FIG. 2. The Feynman diagram for $D^0 \to K^0\bar{K}^0$.

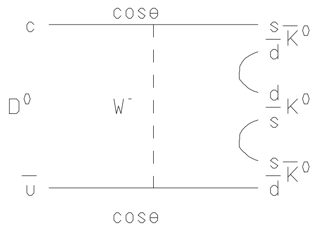

FIG. 3. The Feynman diagram for $D^0 \to K^0_S K^0_S K^0_S$.

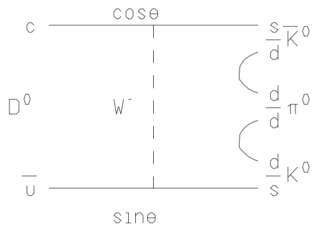

FIG. 4. The Feynman diagram for $D^0 \to K^0_S K^0_S \pi^0$.

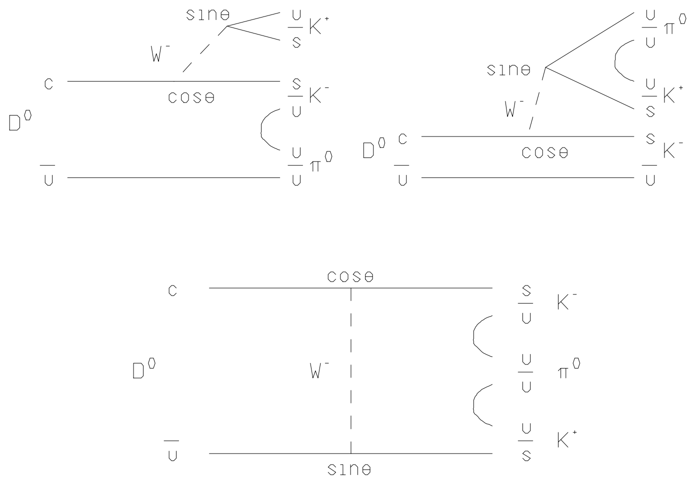

FIG. 5. The Feynman diagram for $D^0 \to K^+ K^- \pi^0$.

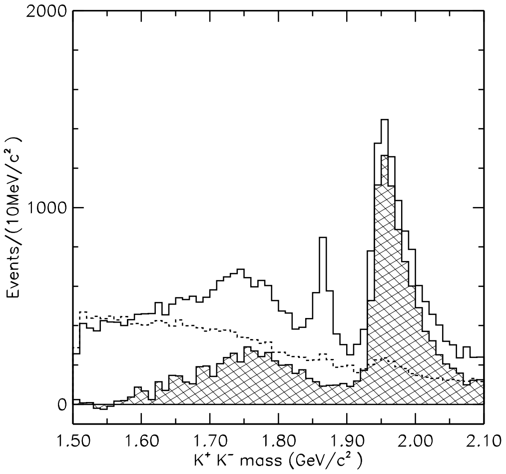

FIG. 6. The K^+K^- invariant mass distribution. The solid line is the D^0 mass signal in the mass difference signal region. The dashed line is background from the mass difference sideband region. The cross-hatched line is the background from the other continuum decay modes, which is calculated using Monte Carlo simulation of continuum hadron production. We see the peak around 1.98 GeV/c^2 due to the misidentified $D^0 \to K^-\pi^+$ events.

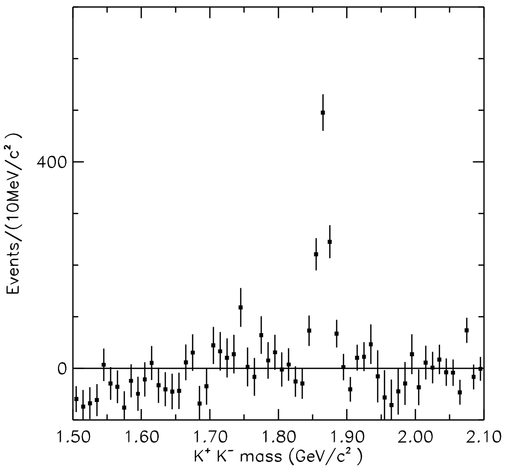

FIG. 7. The reconstructed K^+K^- invariant mass distribution after subtracting all the backgrounds.

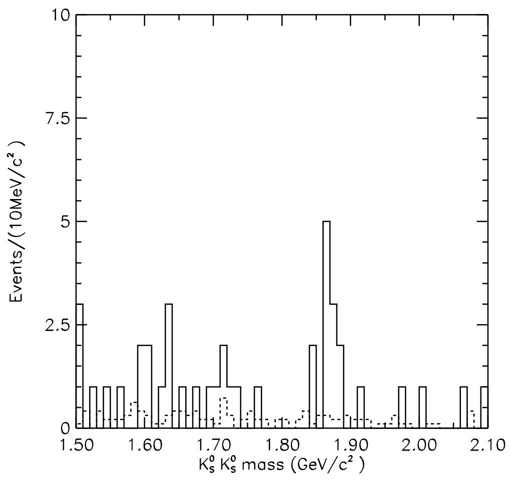

FIG. 8. The invariant mass distribution for $K_S^0 K_S^0$ for the $D^{*\pm}$ tag. The solid line is the D^0 mass signal in the mass difference signal region. The dashed line is background from the mass difference sideband region.

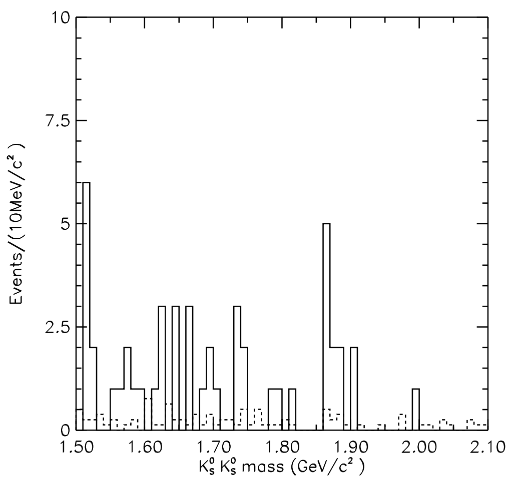

FIG. 9. The invariant mass distribution for $K_S^0 K_S^0$ for the D^{*0} tag. The solid line is the D^0 mass signal in the mass difference signal region. The dashed line is background from the mass difference sideband region.

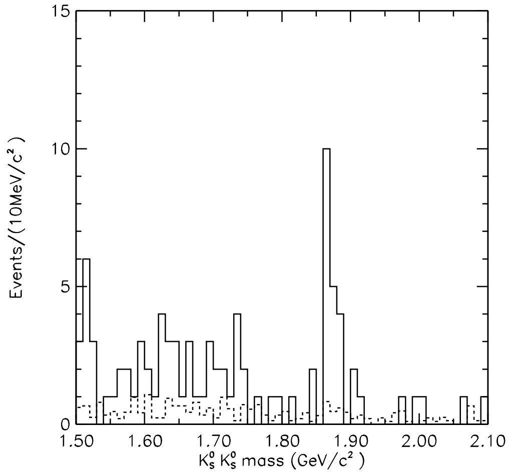

FIG. 10. The sum of the invariant mass distributions for $K_S^0 K_S^0$ for the $D^{*\pm}$ tag and D^{*0} tag data. The solid line is the D^0 mass signal in the mass difference signal region. The dashed line is background from the mass difference sideband region.

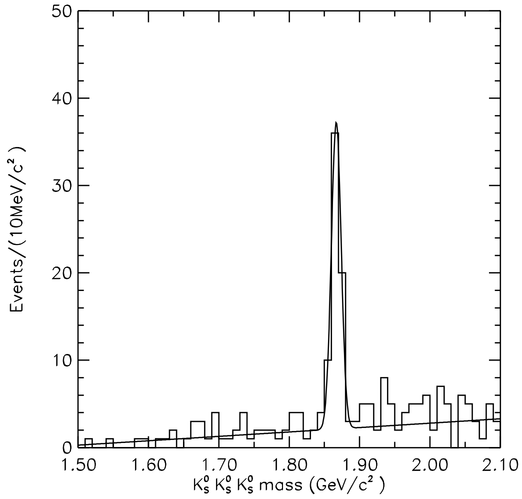

FIG. 11. The invariant mass distribution of $K_S^0 K_S^0 K_S^0$. The signal is fitted by a Gaussian while the background is fitted by Chebyshev polynomial of Order 1.

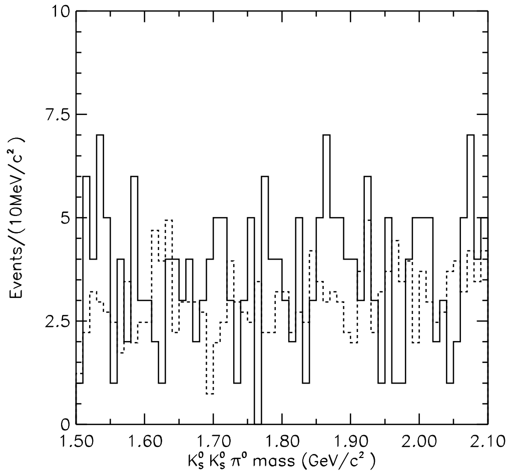

FIG. 12. The invariant mass distribution of $K^0_S K^0_S \pi^0$. The solid line is the D^0 mass signal in the mass difference signal region. The dashed line is background from the mass difference sideband region.

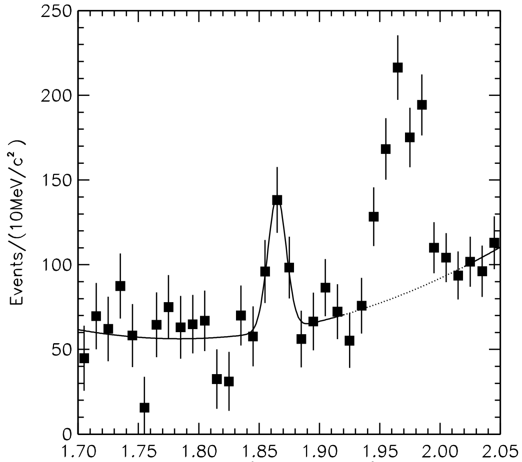

FIG. 13. The invariant mass distribution of $K^+K^-\pi^0$ after doing the normalized mass difference sideband subtraction. In fitting, we exclude the region between 1.92 and 2.02 due to an excess of misidentified $D^0 \to K^-\pi^+\pi^0$ events.

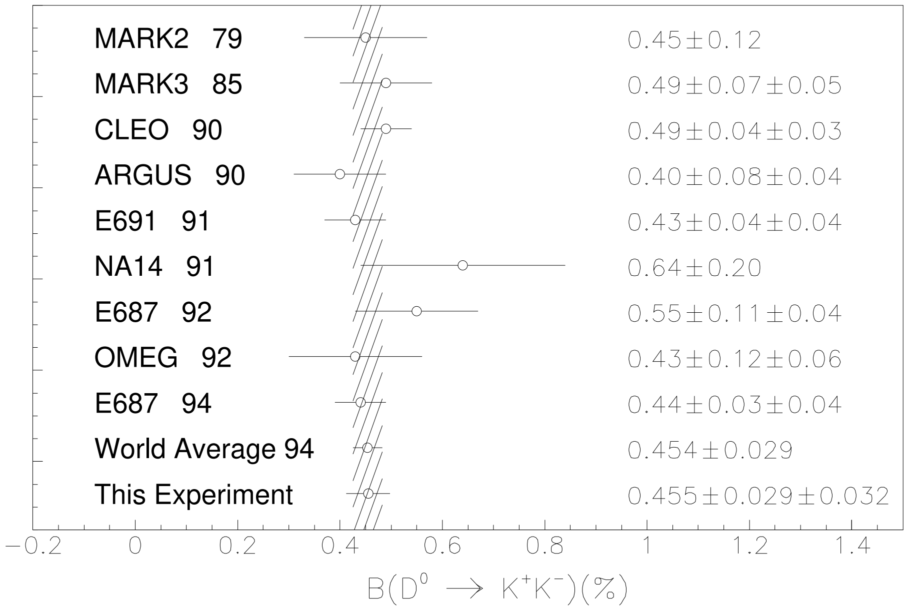

FIG. 14. The previous measurements and our result for the $B(D^0 \to K^+K^-)$ channel.

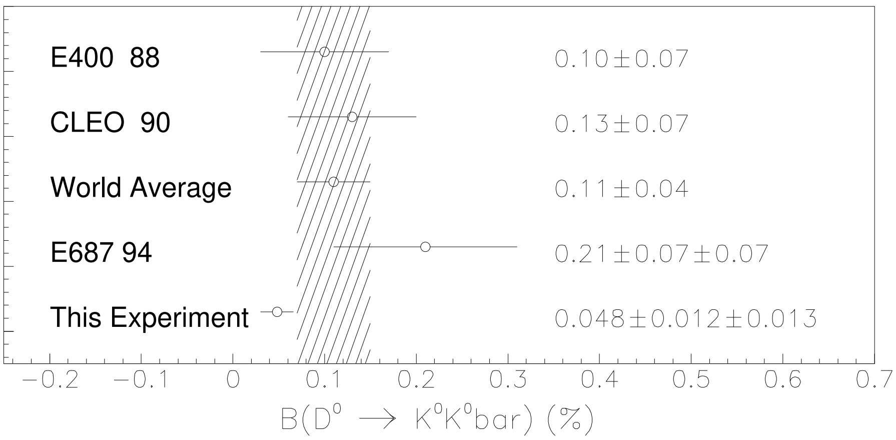

FIG. 15. The previous measurements and our result for the $B(D^0 \to K^0\bar{K}^0)$ channel.

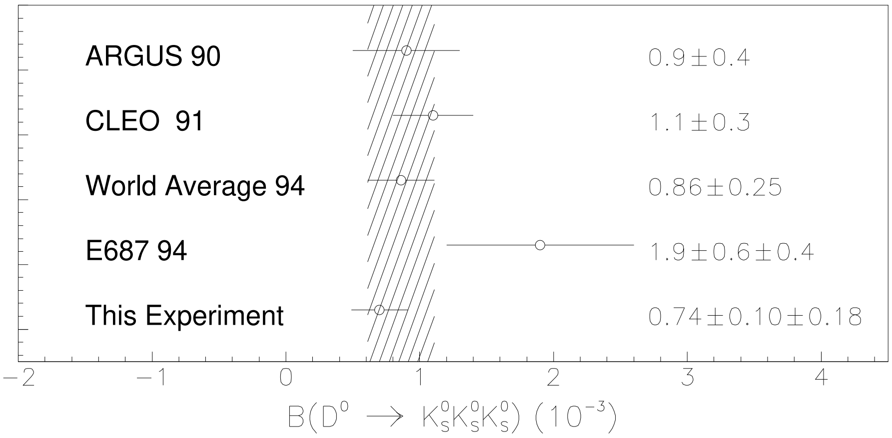

FIG. 16. The previous measurements and our result for the $B(D^0 \to K_S^0 K_S^0 K_S^0)$.